

A Crowd Motion Analysis Framework Based on Analog Heat-Transfer Model

Yu Liang^a, William Melvin^b, Shane Fernandes^a, Michael Henderson^a, Subramania I. Sritharan^c, Darrell Barker^d

^aDept. of Mathematics and Computer Science, Central State Univ., OH, USA

^bSensors and Electromagnetic Applications Laboratory, Georgia Institute of Technology, GA, USA

^cDept. of Water Resource, Central State Univ., OH, USA

^dU.S. Air Force Research Laboratory, OH, USA

Abstract – Crowd motion analysis covers the detection, tracking, recognition, and behavior interpretation of a target group according to persistent surveillance video data. This project is dedicated to developing and employing a generic crowd motion analysis framework, which is based on an analog-heat-transfer model and thus denoted as CMA-AHT for simplicity, to measure and identify the anomalous pedestrians from persistent surveillance video data. Based on the hypothesis of ergodicity, the CMA-AHT framework is formulated according to the statistical analysis about the historical records of crowd's behavior, geographic information system, and crowd motion dynamics. The derivation of the CMA-AHT framework and the innovative methods involved in the framework's implementation will be discussed in detail. Using the sample video data collected by Central Florida University as a benchmark data, CMA-AHT is validated through measuring and identifying anomalous personnel or group in the video.

Key Words – crowd motion analysis, heat-transfer, partial differential equations, geographic information, statistics, video processing

I. Introduction

It is an extremely computationally intense, labor-intensive and highly unreliable job to obtain a panoramic, timely, trusted understanding about crowd behavior [1-5,7,9,14-17,19,23-25,27,29] and its future status by exploiting networked sensor assets (autonomous, heterogeneous and multi-layer sensor nodes). This project proposes a new crowd motion analysis framework, which is mainly constructed over an analog-heat-transfer model [13,18] and denoted as CMA-AHT for simplicity, to detect, track, understand and evaluate pedestrians' activity using persistent surveillance video data [6,8,10,14].

Crowd motion analysis (CMA) is critical for effective surveillance. It plays a significant role in human society. For example, in the area of homeland security, it is a challenging issue to detect and

recognize those anomalous behaviors in crowd scenes (Figure 1) according to their motion features such as velocity, position and trace. In the area of civil engineering, CMA will guide us in making reasonable evacuation plans for use during an emergency. And in the area of city property management, CMA will help policy makers to optimize the exploitation of public resource.



Fig. 1 Observe and detect anomalous behavior in crowd scenes

Crowd motion modeling and simulation have been discussed in many previous works. The existing crowd motion analysis methods are classified into the following three classes of schemes: microscopic [4, 12, 25], macroscopic [14,15,17,19,20,23,24,29], and multi-scale [2].

Microscopic methods regard crowds as consisting of discrete individuals (or agents) so that the movement of each individual within the group can be identified. Microscopic methods provide a very detailed and accurate formulation about crowd's movement while suffering terribly from inhibitive computational cost. Multi-scale methods aim to provide a seamless coupling between a microscopic scheme and a macroscopic scheme.

Macroscopic methods regard pedestrian crowd as a continuum [18]. The macroscopic CMA methods are further divided into anisotropic [15, 29] and isotropic strategies [13, 17, 19]. Being applicable in both anisotropic and isotropic senior, CMA-AHT employs an analog-heat-transfer model to formulate the expected macroscopic movement of crowd in macroscopic way. Compared to alternative methods, the CMA-AHT model uses the pseudo temperature gradient, which is obtained by solving the heat-

transfer-analog partial differential equations, to represent the normal “movement trend” of pedestrians. In the implementation of CMA-AHT framework, the pseudo temperature is not explicitly defined but implicitly given by its gradient.

As a cutting-edge technology in scientific modeling and simulation, multi-scale model is dedicated to seamlessly merge the discrete individual (or particle) behavior with the continuous crowd (or continuum) behavior. It will be a major topic in our future work.

This paper emphatically discusses the following topics: (1) processing and analysis of persistent surveillance video data so as to extract the movement features of target-of-interest; (2) infrastructure of sensor-oriented applications such as crowd-motion analysis based on persistent surveillance video; (3) mathematical modeling of the expected behavior of target-of-interest. The discussions about these topics comprise the major contributions of this work.

This paper is organized as follows: Section II provides a system overview; Section III (pre-processing) discusses how to obtain pedestrian moving status such as the real-time velocity, position and movement trace using persistent surveillance video data; Section IV discusses the formulation of the pseudo temperature field according to a location’s historical crowd motion data; Section V discusses how to use the pseudo-temperature field to measure and analyze the motion of an individual or crowd; Section VI introduces a macro-cell strategy, a variance of divide-and-conquer method, into the CMA-AHT model so that large-scale crowd-motion (such as a city or even a country) can be simulated efficiently. Section VII summarizes the effort.

II. Overview of the Implementation of CMA-AHT framework

As illustrated in Figure 2, CMA-AHT couples three modules: (1) crowd motion dynamics, (2) geographic information, and (3) processing and analysis of persistent surveillance video data. In other words, crowd motion dynamics, geographic information, and video data constitutes the three inputs of CMA-AHT model.

Considering the prohibitive cost to obtain accurate “situational awareness” from sensor networks [8], the proposed CMA-AHT framework for data fusion, manipulation, and prediction is supposed to own the following features:

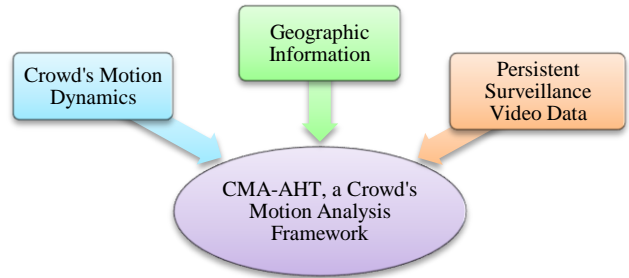


Fig. 2 Infra-structure of the CMA-AHT framework: a coupling of GIS, video data and motion dynamics

- All related data will be merged into a single shared platform. The CMA-AHT platform should provide interfaces to a variety of sensor carriers such as satellite, unmanned vehicle/flight, and on-ground cameras, etc. and be capable of handling heterogeneous sensory data such as hyper-spectral image/video and radar/LADAR signal [27, 28], etc. Putting those heterogeneous data, which might have different spatial and temporal scale and be of different format, on a single platform will help us to obtain a comprehensive situational awareness about ongoing pedestrian behavior. In addition, a single shared platform can easily coordinate cooperative sensor nodes.
- The expected or normal crowd behavior is mathematically formulated as temporal- and spatial-dependent partial differential equations (PDE) [13], which is derived from the statistical analysis on historical sensory data. Using the partial differential equations as reference, situational awareness about the observed pedestrian individual or crowd can be obtained.
- According to its current situational knowledge about crowd motion, the CMA-AHT platform will deliberately collect more detailed and specific sensory data for further analysis (we call this data scavenging or self-optimization). For example, if an anomalous pedestrian motion is detected, CMA-AHT will “zoom-in” for further detailed information corresponding to the target-of-interest, contextualized by already available relevant data. On the other hand, the non-dominant or redundant information corresponding to the target-of-interest will be ignored. The optimization of the exploitation of sensor data according to existing situational awareness is called “self-optimization”.
- Besides the “self-optimization” function, according to current situational awareness, CMA-AHT should be able to collectively control the parameters of autonomous sensor nodes for a better observation about the target-of-pedestrian.

Self-optimization of the exploitation of sensory data and the collective control of sensor asset will be discussed in our future work.

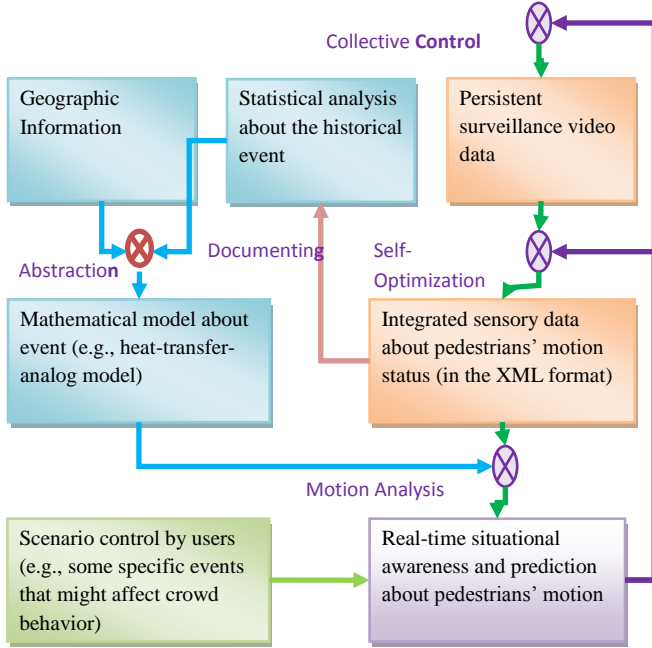


Fig. 3 Flow-chart of crowd motion analysis

Figure 3 describes the flowchart of CMA-AHT framework. It is illustrated that the implementation of CMA-AHT consists of following two threads:

- Formulating the pseudo-temperature field using historical motion data about crowd activity in the scene.
- Obtaining the motion features (velocity, location, number of pedestrians, etc.) by processing the persistent surveillance video data. The implementation of each thread will be discussed in this paper.

Based on the above two threads, a situational awareness about the behavior of observed pedestrians can be measured and evaluated. A detailed description about the implementation of the above two threads and their application in motion measurement and analysis will be covered in the following three sections.

III. Processing of Video Data

3.1 Overview of Video Processing

In this work, video data processing aims to extract a pedestrian’s motion features, to include velocity, position, and motion trace, out of the persistent surveillance video data.

Processing of persistent surveillance video data includes the following operations: (1) acquisition of video data; (2) segmentation, which extracts pixels of pedestrians from background; (3) isolation of pedestrians out of noise or other moving objects; (4) translation of optical moving features (i.e., the velocity and position of moving targets within the sensor coordinate system) of detected pedestrians into their actual moving features (i.e., the velocity and position of moving targets within the geographic coordinate system); (5) documentation, which posts the output in a format suitable for post-processing and includes position, velocity, and track (optional). Step (3) and (4) will be emphatically discussed in this section.

Table 1 lists the notations involved in the processing of video data. As addressed in the “Annotation” column of the table, the specifications about the camera are predetermined. The expected human dimension $\langle w, l \rangle$ is derived from the statistical analysis about human body. The optical moving features, which include the position of target in the frame (x_{sensor}, y_{sensor}) and velocity derived from video sequence $(v_{sensor,x}, v_{sensor,y})$ using optical-flow algorithms [6]. Based on the above parameters, the moving features about pedestrians,

Table 1: Notations involved in the processing of video data

Variables		Definition	Annotation
Specif. about the electro-optical camera	ϕ_0	The angle between vertical and optical axis	Pre-determined
	f	Focus length	
	h	The altitude of lens from the ground	
	$(\alpha_{max}, \beta_{max})$	Maximal view angle of camera lens	
	$P_{totalView}$	Total pixel area of video frame	
Expected dimension of target	$\langle w \rangle$	Expected width about target	User defined
	$\langle l \rangle$	Expected height about target	
	P_{target}	Pixel area of expected target	Derived from the expected target dimension and lens specif.
Optical moving features of target	(x_{sensor}, y_{sensor})	Position of target in video frame	Directly derived from video sequence using optical algorithms
	$(v_{sensor,x}, v_{sensor,y})$	Optical velocity of target in video frame	
Geographic moving features of target	(x, y)	Geographic position of target (Figures 4 and 5)	To be calculated using optical moving feature and lens specif.
	(v_x, v_y)	Geographic moving velocity of target (Figures 4 and 5)	

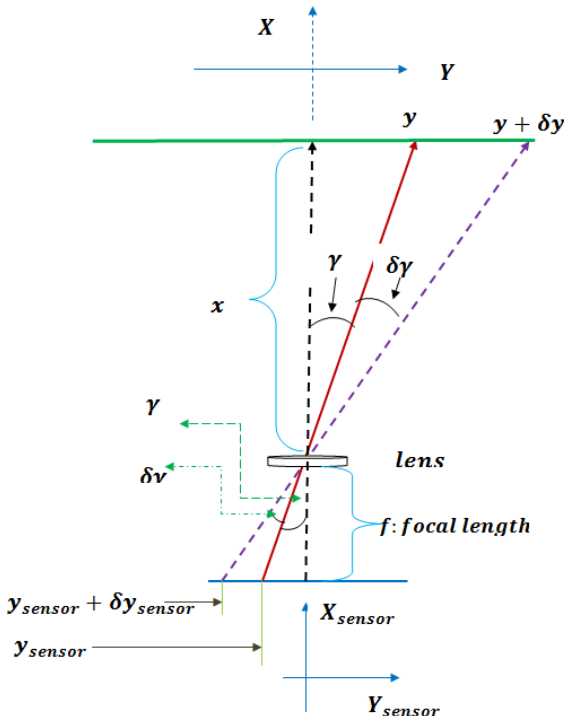


Fig. 4 Side-view of the sensor coordinate system and geographic coordinate system

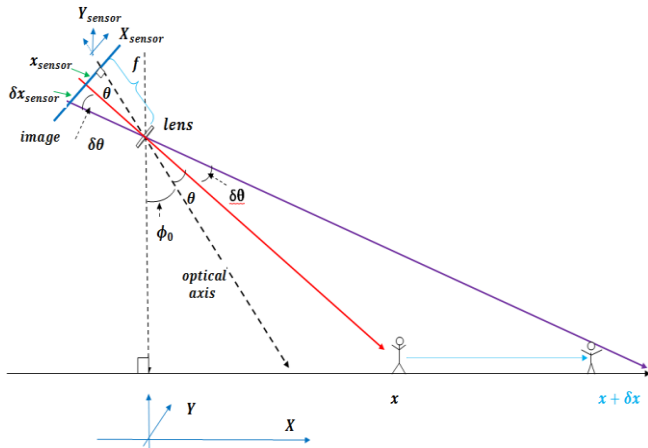


Fig. 5 Overview of the sensor coordinate system and geographic coordinate system

which include geographic position and geographic velocity, can be calculated.

Figures 4 and 5 provide a vivid illustration about the key notations involved in video processing.

3.2 Acquisition of Video Data

This effort supports multiple collaborative input-equipment. The resulting data will be collected and fused by CMA-AHT server.

In this work, the persistent surveillance video data comes from benchmark data collected by the University of Central Florida (www.ucf.edu/data).

3.3 Segmentation of Target-of-Interest

In this work, segmentation is accomplished using the optical-flow method [6,10] and the background-subtraction method [6,10] jointly. Optical-flow is used to segment those pixels corresponding to the moving targets or pedestrians. Background subtraction method is used to segment those pixels corresponding to the still targets or pedestrians.

3.4 Isolation of Target-of-Interest According to Their Expected Pixel Area

The pedestrian objects are detected by clustering those pixels with similar motion features. At this step, estimation about the pixel area (or the dimensional size) of the targeting pedestrian, which is denoted as P_{target} , is needed due to the following two motivations:

- Firstly, P_{target} will help us identify the targets from those too big (e.g., moving vehicle) or too small objects (e.g., noise).
- Secondly, when several targets are clustered together closely, P_{target} can help us obtain the number of pedestrians.

In this work, P_{target} , the expected pixel area about target is calculated via the following equations:

$$P_{target} = \frac{\alpha\beta}{\alpha_{max}\beta_{max}} P_{totalView} \quad (1)$$

where

$$\begin{cases} x = h \left[\frac{f \tan(\phi_0) + x_{sensor}}{f - \tan(\phi_0)x_{sensor}} \right] \\ \alpha = \sin^{-1} \left(\frac{x}{\sqrt{x^2 + (h - \langle l \rangle)^2}} \right) - \sin^{-1} \left(\frac{x}{\sqrt{x^2 + h^2}} \right) \\ \beta = 2 \tan^{-1} \left(\frac{\langle w \rangle}{2\sqrt{x^2 + h^2}} \right) \end{cases} \quad (2)$$

and the parameters involved in Equation (1) and (2) are defined in Table 1.

The above formula for P_{target} is validated using the real pixel-area about targeting pedestrian, which is illustrated in Figure 6.

Figure 7 illustrates a comparison between the theoretical pixel-area defined by Eq. (1) and real pixel area about targeting pedestrians. It is observed that theoretical pixel-area is basically consistent with the real pixel-area about targeting pedestrians. It should be

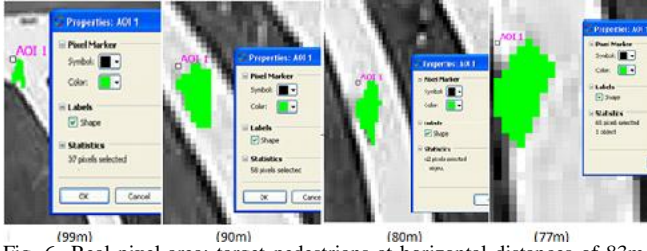


Fig. 6 Real pixel-area: target pedestrians at horizontal distances of 83m-193m from camera have variant pixel-area ranging from 34 pixels to 116 pixels (83m)

remarked that the theoretical pixel-area is derived from the following configurations: the view angle limit $(\alpha_{max}, \beta_{max})$, pixel-area of the whole frame $P_{totalView}$, the altitude of lens from the ground h , and the expected human dimension $(<l>, <w>)$. It is observed that:

- Eq. (1) provides a very accurate estimation about the pixel-area of target pedestrians.
- Instead of the distance between target and lens, the pixel-area of a target pedestrian is mainly dependent on the view angle about target.
- Target pedestrians at horizontal distances of 83m-193m from camera have variant pixel-area ranging from 34 pixels to 116 pixels (83m).

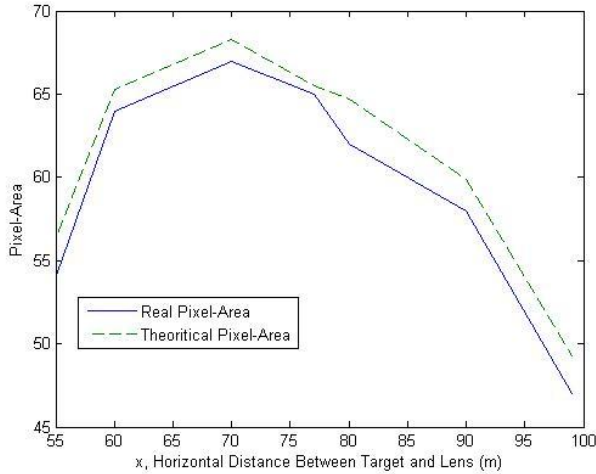


Fig. 7 Validation of the expected pixel-area about target pedestrian, with view-angle limit $\alpha_{max} = 33.5^\circ$ by $\beta_{max} = 40.8^\circ$, pixel-area of the whole frame $P_{totalView} = 1024 * 768(pixel)$, expected human dimension $<l> = 1.7m$ by $<w> = 0.66m$, and the altitude of lens from the ground $h = 44.2m$

3.5 Translating the Optical Velocity into Geometrical Velocity

Through the detection step, the optical velocity $(v_{sensor,x}, v_{sensor,y})$ and the optical position (x_{sensor}, y_{sensor}) of each pedestrian or pedestrian block

(sometimes the pedestrians are too close to be identified) are obtained.

In the following step, it is necessary to obtain the geographic motion feature (i.e., (x, y) and (v_x, v_y)) of pedestrians according to the optical motion features (i.e., $(v_{sensor,x}, v_{sensor,y})$ and (x_{sensor}, y_{sensor})). As illustrated in Figures 4 and 5, optical motion features are formulated within the sensor coordinate system (X_{sensor}, Y_{sensor}) and geographic motion features are formulated within the geographic coordinate system (X, Y) .

Geographic motion feature are computed according to the pre-determined specifications of the video camera and the observed optical motion feature. From Figures -5 and the following trigonometry formula:

$$\tan(\alpha + \beta) = \frac{\tan(\alpha) + \tan(\beta)}{1 - \tan(\alpha)\tan(\beta)} \quad (3)$$

(x, y) is computed via the following formula:

$$\begin{cases} x = h \tan(\phi_0 + \theta) = h \left[\frac{f \tan(\phi_0) + x_{sensor}}{f - \tan(\phi_0)x_{sensor}} \right] \\ y = x \tan(\gamma) = \frac{h}{f} \left[\frac{f \tan(\phi_0) + x_{sensor}}{f - \tan(\phi_0)x_{sensor}} \right] y_{sensor} \end{cases} \quad (4)$$

Furthermore, Figures 4 and 5 illustrates that:

$$\begin{cases} x + \delta x = h \tan(\phi_0 + \theta + \delta\theta) \\ y + \delta y = x \tan(\gamma + \delta\gamma) \end{cases} \quad (5)$$

According to the trigonometry formula (1) and limit theory, it follows that

$$\begin{aligned} v_x &= \lim_{\delta t \rightarrow 0} \frac{\delta x(t)}{\delta t} = \lim_{\delta t \rightarrow 0} \frac{h \tan(\phi_0 + \theta + \delta\theta) - x}{\delta t} \\ &= \lim_{\delta t \rightarrow 0} \frac{h}{\delta t} \left\{ \frac{f \tan(\phi_0) + x_{sensor} + v_{sensor,x} \delta t}{f - \tan(\phi_0)(x_{sensor} + v_{sensor,x} \delta t)} \right. \\ &\quad \left. - \frac{f \tan(\phi_0) + x_{sensor}}{f - \tan(\phi_0)x_{sensor}} \right\} \end{aligned} \quad (6)$$

and

$$\begin{aligned} v_y &= \frac{x(t)}{f} v_{sensor,y} \\ &= \frac{h \tan(\phi_0 + \theta)}{f} v_{sensor,y} \end{aligned} \quad (7)$$

Following Equations (6) and (7), (v_x, v_y) can be formulated using the following formula:

$$\begin{cases} v_x = \left[\frac{h}{f - \tan(\phi_0)x_{sensor}} \right] v_{sensor,x} \\ v_y = \left[\frac{h(f \tan(\phi_0) + x_{sensor})}{f(f - \tan(\phi_0)x_{sensor})} \right] v_{sensor,y} \end{cases} \quad (8)$$

3.6 Documenting Video Processing Results

All the pre-processing results are stored in XML-format. XML-format pre-processing data consists of (1) camera data, and (2) pedestrian data. As illustrated in Figure 3, those data will be stored and employed to formulate the mathematical model of the pedestrians' motion.

IV. Mathematical Description of CMA-AHT Model

4.1 Governing Equations for CMA-AHT Model

The mathematic model for crowd motion is formulated based on the hypothesis of ergodicity [7,13,25,26], which indicates that a dynamical system has the similar (or periodic) behavior averaged over time as averaged over the space of all the system's states.

The governing equation for the CMA-AHT model is given in Formula (9):

$$C(X) \frac{\partial T(X,t)}{\partial t} + \nabla \cdot (-K(X) : \nabla T(X,t)) = Q(X) \quad (9)$$

It is observed that the CMA-AHT model shares similar governing equations with the canonical heat-transfer model [18,19,20] while having a different physical explanation for this application. In equation (9), X indicates the position of pedestrian; t indicates the time; $C(X)$ indicates the pedestrian capacity at location X ; pseudo thermal conductivity tensor $K(X)$ indicates the pedestrian throughput that is derived from the historical crowd motion data, for example, grassland should have smaller $\|K(X)\|$ (i.e., the norm of tensor) value compared to that of a walkway; $Q(X)$, the pseudo energy per unit volume generated per unit time, indicates the normal behavior initiated within the scene; and pseudo temperature $T(X,t)$ indicates the empirical crowd's pseudo kinetic energy density.

An explicit quantitative definition about pseudo temperature $T(X,t)$ is not given in this work because the value of pseudo temperature itself is not our concern. Quantitatively, $T(X,t)$ is implicitly defined through the definition about its gradient $\nabla T(X,t)$:

$$K(X) \nabla T(X,t) = \left\langle \sum_i m_i v_i \right\rangle \quad (10)$$

In above equation, $\left\langle \sum_i m_i v_i \right\rangle$ indicates the expected collective momentum ($m_i = \text{mass}$, $v_i = \text{velocity}$) of the crowd. $\nabla T(X,t)$ will be employed to measure and analyze the motion of pedestrians.

Similar to a canonical heat-transfer model, which is derived from the law of conservation of energy and Fourier's law, CMA-AHT model is derived from the law of conservation of the crowd's pseudo kinetic energy, Fourier law, and the following extra assumptions.

- Anomalous action does not initiate within a boundary cell (i.e., an image is divided into a grid of scene and boundary are located at the edges of image).
- Normal behavior initiated within the boundary cell can be modeled by $Q(X)$, the pseudo-energy generated within the scene.
- Crowd motion has Gaussian distribution [11].

According to the law of conservation of crowd's pseudo-kinetic energy, where the rate of change of pseudo-kinetic energy should be equal to the sum of pseudo-energy flow across the boundary per unit time and pseudo-energy generated inside per unit time:

$$\frac{\partial T(X,t)}{\partial t} = \nabla \circ f(X,t) + Q(X) \quad (11)$$

Furthermore, based on the assumptions that (1) an entering pedestrian contributes positive kinetic energy; (2) an existing pedestrian contributes negative kinetic energy, Fourier's Law also holds true because a dominant number of pedestrians will move from a high energy position to a low energy location. Therefore,

$$f(X,t) = -K(X) \nabla T(X,t) \quad (12)$$

In CMA-AHT model, the kinetic flow of the crowd is quantitatively defined as the expected value of the collective crowd moment during a specific time period $[t - \Delta t, t + \Delta t]$:

$$f(X,t) \{X \in \Gamma_1\} = \left\langle \sum_{\substack{\tau \in N, X \in \Gamma_1, \tau \in [t - \Delta t, t + \Delta t]}} m_i v_i(X, \tau) \right\rangle \quad (13)$$

Coupling Equations (11) and (12), the governing equation (9) for the CMA-AHT model is formulated. In this paper, the CMA-AHT model only discusses two-dimensional problems, where the governing equation becomes:

$$C(x, y) \frac{\partial T(x, y, t)}{\partial t} = \frac{\partial}{\partial x} (K_x \frac{\partial T(x, y, t)}{\partial x}) + \frac{\partial}{\partial y} (K_y \frac{\partial T(x, y, t)}{\partial y}) + Q(x, y) \quad (14)$$

It should be emphasized that in most cases K_x does not have to be equal to K_y because in reality the crowd motion is anisotropic. Given appropriate boundary conditions, Equation (14) can be solved using suitable numerical methods (e.g., finite difference or finite element) and finally ∇T , the pseudo temperature gradient, will be obtained.

The following section will focus on the formulation of physics domain Ω and boundary conditions.

4.2 Geometry Configuration of CMA-AHT

To formulate the mathematics model of CMA-ATH, the physics domain Ω for pseudo temperature field is directly derived from the geographic information system such as Google-Earth in this work. As an alternative way, an accurate geometrical configuration should be generated using image vectorization software.

4.3 Boundary Conditions Formulation for CMA-AHT

Once the geometry configuration of the CMA-AHT model is formulated, the temperature field about it will be determined with sufficient boundary conditions.

The boundary conditions for the CMA-AHT model are formulated based on the following assumptions:

- The crowd motion is periodic, either daily, weekly or corresponding to special event;
- The crowd motion is Gaussian-distributed.

Table 2: sample historical motion data around t=9:00am

DATE	(x, y)	(v _x , v _y)	ANNOTATION
1998.7.3, 8:59am	(345m, 200m)	(-5.0m/s, 6.0m/s)	*
1998.7.3, 9:01am	(215m, 120m)	(1.5m/s, 2.6m/s)	*
1998.7.4, 8:58am	(125m, 100m)	(2.0m/s, 3.3m/s)	Event (Firework)
1998.7.4, 9:02am	(-111m, 200m)	(0.5m/s, 0.2m/s)	Event (Firework)
...
2011.7.5, 9:00am	(-32m, 215m)	(2.5m/s, 7.0m/s)	*

As a result, the boundary conditions for CMA-AHT model are directly derived from the historical

pedestrians' motion record. For example, to formulate the temperature field at 9:00am, we can employ the historical pedestrians' motion data during time period [9.0-0.1, 9.0+0.1] (illustrated in Table 2).

The boundary conditions for CMA-AHT model consist of Neumann boundary conditions and Dirichlet boundary conditions [18,21,22].

Neumann boundary conditions ($\Gamma_1 \subseteq \partial\Omega$) indicates expected collective momentum that moves across boundary Γ_1 during the period $[t-\Delta t, t+\Delta t]$. In this work, Neumann boundary condition is defined by the following formula:

$$-K\nabla T(X, t) \{X \in \Gamma_1\} = \left\langle \sum_{i \in N, X \in \Gamma_1, \tau \in [t-\Delta t, t+\Delta t]} m_i v_i(X, \tau) \right\rangle \quad (15)$$

Dirichlet boundary conditions ($\Gamma_2 \subseteq \partial\Omega$) indicate pseudo kinetic energy.

$$T(X, t) \{X \in \Gamma_2\} = T_0 \quad (16)$$

In CMA-AHT model, Dirichlet boundary conditions are only used to ensure the non-singularity of the governing equations. In Formula (16), T_0 is a meaningless arbitrary value.

Figure 9 shows the Neumann boundary (Γ_A, Γ_B and Γ_C) and Dirichlet boundary (T_0) conditions that are derived from the historical crowd motion data at around 9:00am, which is illustrated in Figure 8. It should be remarked that Neumann boundary conditions are effective only when there is dominant number of entry targets or exit targets.

A finite element method [18,21,22] is used to solve the governing equation (9) with Neumann and Dirichlet boundary conditions. Figures 10 (a) and (b) shows the resulting pseudo-temperature field and the temperature gradient, from which the expected motion velocity of crowd is illustrated.

V. Measuring the Motion of Pedestrians Using Pseudo Temperature Field

The last section mainly discusses the details of the formulation of the pseudo temperature field. In this section, the resulting temperature field will be used to measure and evaluate the motion of an individual pedestrian and a crowd.

5.1 Quantitative Measurement of a Pedestrian's Movement

Assuming that a pseudo temperature field for a specific location (X) and time-period ($[t-\Delta t, t+\Delta t]$) has been formulated and thus the resulting pseudo-



Fig. 8 Historical crowd motion status at around 9:00am

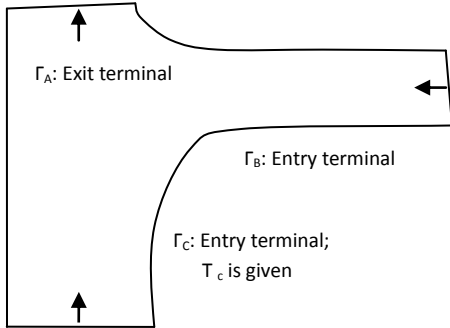


Fig. 9 Boundary conditions derived from historical data around 9:00am

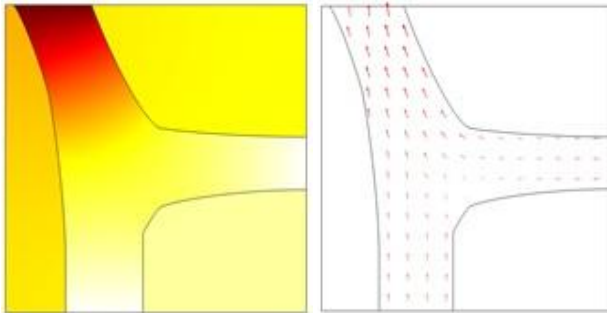


Fig. 10 Pseudo temperature field around 9:00am: (a) pseudo temperature field; (b) pseudo temperature gradient

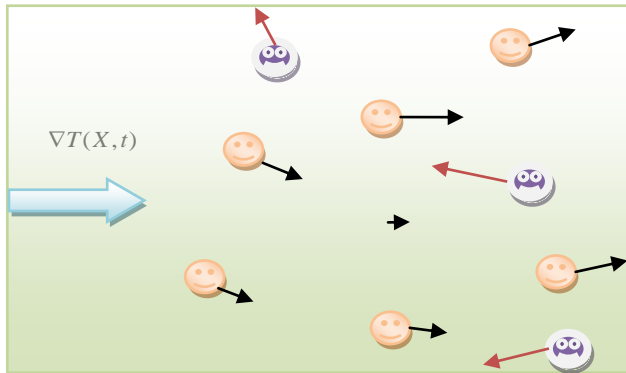


Fig. 11 Pedestrian motion within the CMA-AHT pseudo-temperature field temperature-gradient $\nabla T(X,t)$ is known, then a pedestrian at similar location and time-period with observed velocity $v(X,t)$ can be measured by the ζ -value. , which is defined using following formula:

$$\xi(t) = \nabla T(X,t) \circ v(X,t) \tag{17}$$

In Formula (17), “ \circ ” indicates inner-product.

Figure 11 shows that a crowd of pedestrians move within a pseudo temperature field, where the pseudo temperature gradient $\nabla T(X,t)$ is indicated by big arrow. The small arrows indicate the observed moving velocity of the individuals. Using Formula (17) we can obtain the ζ -value of each pedestrian. It is observed that the pedestrians in the diagram are classified by two groups (i.e., smiling faces and angry faces) with reference to $\nabla T(X,t)$. As illustrated in Figure 11, the “smiling face” indicates the pedestrian whose moving direction is compatible with the expected crowd’s moving direction, which is derived from the historical data. The “angry face” indicates the pedestrian whose moving direction conflicts with the expected moving direction.

5.2 Measurement of a Pedestrian’s Movement with Reference to the Neighboring Pedestrians in the Scene

Given the pseudo temperature field, pedestrians can be categorized according to their ζ -value. Figure 12 shows the ζ -value histogram of a group of pedestrians. Circles A and C indicate the anomalous pedestrians who move faster than others. Circle B indicates the anomalous pedestrians who stand still or move in the direction orthogonal to $\nabla T(X,t)$.

Figures 13 and 14 show that, with reference to the pseudo temperature field formulated in Figure 10, the pedestrians in the scene at around 9:00am can be categorized into the positive- ζ -value and negative- ζ -value groups. The latter group of pedestrians is regarded as anomalous because only minority of pedestrians in the scene during that period has negative ζ -value.

Furthermore, according to formula (17), the motion of a group of people can be accessed using the following formula:

$$\Psi = \sum_{i=1}^n \xi_i = \sum_{i=1}^n (\nabla T(X_i,t) \circ \vec{v}_i)$$

where n indicate the number of people of the group.

5.3 Quantitative Measurement of Pedestrians’ Movement during Specific Time Period

The movement of a pedestrian during a specific time period can be also measured according to the time-sequence of ζ -value.

Figure 15 shows the sample time-sequence of ζ -

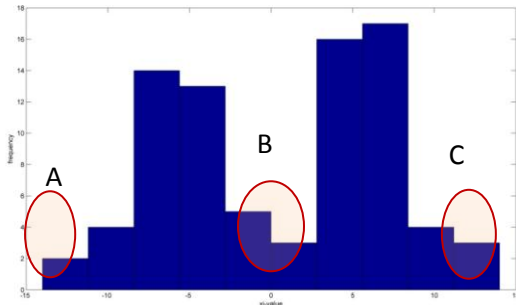


Fig. 12 Histogram of ζ -value of pedestrians



Fig. 13 Normal pedestrians (with positive ζ -value, squared in green-color) appeared in the scene at around 9:00am



Fig. 14 Anomalous pedestrians (with negative ζ -value, squared in red-color) appeared in the scene at around 9:00am

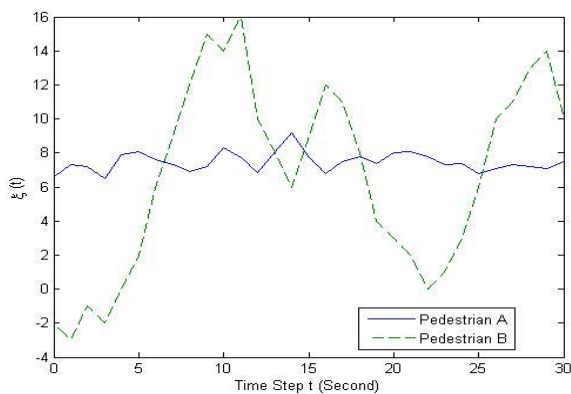


Fig. 15 ζ -value about two sampling pedestrians in 30 seconds period

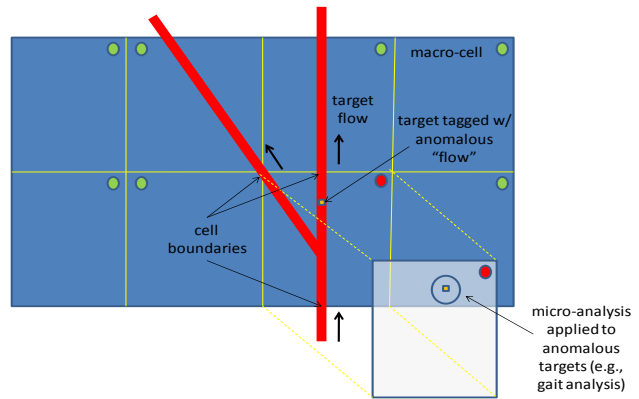


Fig. 16 Enhanced CMA-AHT model: using macro-cell strategy to analyze crowd-behavior within a large-scale scene (the red lines indicate pathways), which is partitioned into multiple non-overlapping subdomain

value about two pedestrians --Pedestrian A and Pedestrian B within thirty seconds. It is observed that Pedestrian B has a larger ζ -value fluctuation than Pedestrian B. Due to his/her super inconsistent moving behavior, Pedestrian B is regarded as a relatively anomalous pedestrian.

VI. Using Macro-Cell Strategy to Handle Large-Scale Scene

Instead of only a street block, crowd motion analysis might be needed in a large scene such as a community, a city or even a country. As a result, a CMA-AHT framework should be scalable so as to solve the large-scale problems.

In our future work, a macro-cell strategy, which partitions the global physics domain into multiple subdomains and then manipulates them independently [21,22], will be employed to enhance the capability of the CMA-AHT framework to handle large-scale problems. As illustrated in Figure 16, each cell will work independently. Inter-cell communications only occur between neighboring cells and they are only triggered while somewhat anomalous crowd behavior is observed and detected.

VII. Summary

This paper develops a sharable self-optimizing and cooperative control sensor network platform for sensor-oriented applications such as persistent surveillance on human behavior and the tracking of environmental phenomenon. As demonstrated in experimental results, the CMA-AHT model can efficiently measure and detect those anomalous individuals within a crowd.

As a multidisciplinary research topic, this work involves image/video processing, partial differential equations, statistics physics, cooperative control, finite-element-method, and optimization, etc., This research integrates the following cutting-edge techniques: processing, analysis, fusion, documenting, compression, storage, and management of heterogeneous sensory data; mathematical modeling of temporal and spatial-dependent (or geographic-dependent) events according to discrete historical observation; evaluation and prediction of observed events according to mathematical modeling of events; full exploitation of the sensor asset according to specific situational awareness; and cooperative control of sensor nodes. Further investigations about these challenging issues need to be made in our future work. This work can be extended to more complicated real-world problems. As a summary, future work includes:

- Introducing stochastic processes to handle uncertainty [26].
- Introducing Lagrange multiplier to handle the influence of geometric constraints (such as train, bus) over the crowd movement.
- Extending the CMA-AHT for three-dimensional scenario.
- Connection with sensor network [8].
- Using macro-cell-based CMA-AHT framework to formulate larger-scale scenes such as community, town or even a city.
- Self-optimization of the exploitation of sensory data and the collective control of sensor asset. Self-optimization will be implemented using principal component analysis (PCA) method. As a cutting-edge research topic in control theory, collective control of sensor asset will also be investigated in our future work.

In addition, the CMA-AHT framework addressed in this paper provides a generic strategy for the processing and analysis of sensory data. Besides crowd-motion analysis, it can be customized and applied in many other sensor-oriented problems such as the simulation of the spread of epidemic disease [20], the management and control of traffic light, prediction of the immigration of locust, etc.

ACKNOWLEDGMENT

This work is jointly sponsored by the National Science Foundation (NSF) with proposal number 1240734, the Air Force Summer Faculty Fellowship Program (SFFP), and the U.S. Air Force Research Lab via contract FA8650-05-D-1912 001702. The authors would like to thank Ms. Olga Mendoza-Schrock of the Sensors Directorate in Air Force

Research Laboratory (AFRL) for her support and guidance of this work. This document is approved for public release by 88 ABW/PA on March 28, 2013 as Document Number 88 ABW-2013-1507.

REFERENCES

- [1] J.K. Aggarwal, J.K., and Cai, Q. (1999). "Human Motion Analysis: A Review". *Computer Vision and Image Understanding*, 73 (3), 428-440.
- [2] AlGadhi, S. and Mahmassani, H. (1991). "Simulation of crowd behavior and movement: Fundamental relations and applications". *Transportation Research Record*, (1320):260-268.
- [3] Al-nasur, S.; Mahmassani, H. (1991). "Simulation of crowd behavior and movement: Fundamental relations and application". *Transportation Research Record*, 1320, 260-268.
- [4] Blue, V. and Adler, J. (1998). "Emergent fundamental pedestrian flows from cellular automata microsimulation". *Transportation Research Record*, 1644:29-36.
- [5] Boulic, R., Thalmann, M.N., and Thalmann, D. (1990). "A global human walking model with real-time kinematic personification". *Visual Computing*, 6, 344-358.
- [6] Bovik, A. C. (2010), "Handbook of image and video processing (2nd Edition)", ISBN: 978-0-12-119792-6.
- [7] Chandler, R.E., Herman, R.; Montroll, E. W. (1958). "Traffic dynamics: studies in car following". *Operations Research*, 6, 165-184.
- [8] Dargie, W. and Poellabauer, C., "Fundamentals of wireless sensor networks: theory and practice", John Wiley and Sons, 2010 ISBN 978-0-470-99765-9, pp. 168-183, 191-192.
- [9] Fan, J., El-Kwae E.A., Hacid M-S, and Liang F. (2002). "Novel tracking-based moving object extraction algorithm". *J. Electron Imaging*, 11, 303.
- [10] Fernandes S., Liang, Y., Sritharan S.I., Wei, X., and Kandiah, R., "Real Time Detection of Improvised Explosive Devices using Hyperspectral Image Analysis", 2010 IEEE National Aerospace and Electronics Conference (NAECON 2010).
- [11] Gardiner, C., "Handbook of stochastic methods: for physics, chemistry & the natural sciences" (Series in synergetics, Vol. 13), (3rd Ed.), ISBN-13: 978-3540208822.
- [12] Gips, P. G. and Marksjo, B. (1985). "A micro-simulation model for pedestrian flows". *Mathematics and Computer in Simulation*, 27:95-105.
- [13] Golubitsky, M., "Introduction to Applied Nonlinear Dynamical Systems and Chaos". New York: Springer-Verlag, 1997.
- [14] Green, R.D., Guan, L., and Burne, J.A. (2000). "Video analysis of gait for diagnosing movement disorders". *J Electron Imaging*, 9, 16.
- [15] Helbing, D. (1992). "A fluid-dynamic model for the movement of pedestrians". *Complex Systems*, 6:391-415.
- [16] Henderson, L. F. (1974). "On the fluid mechanic of human crowd motion". *Transportation research*, 8:509-515.

- [17] Hughes, R. L. (2002). "A continuum theory for the flow of pedestrians". *Transportation Research Part B*, 36:507-535.
- [18] Incropera F. P., "Fundamentals of Heat and Mass Transfer (6th Edition)". ISBN-13: 978-0470055540.
- [19] Liang, Y., Melvin, W., S. I. Sritharan, S. I., Fernandes, S. and Barker, D., "CMA-HT, a Crowd Motion Analysis Framework Based on Heat-transfer-analog Model". *Proc. SPIE 8402, Evolutionary and Bio-Inspired Computation: Theory and Applications VI*, 84020J (May 1, 2012); doi:10.1117/12.919088.
- [20] Liang, Y., Shi, Z.J., Sritharan S. I., and Wan H. (2010). "Simulation of the Spread of Epidemic Disease". COMSOL 2010. Boston.
- [21] Liang, Y, Szularz, M., and Yang, L. T., "Finite-element-wise Domain Decomposition Iterative Solvers Based on Polynomial Preconditioning", DOI: 10.1016/j.mcm.2012.11.017, *Mathematical and Computer Modeling* (in press).
- [22] Liang, Y., Weston, J., and Szularz M., "Generalized least-squares polynomial preconditioners for symmetric indefinite linear equations". *Parallel computing* 28(2): 323-341 (2002).
- [23] Lighthill, M.H., Whitham, G.B.,(1955), "On kinematic waves II: A theory of traffic flow on long, crowded roads". *Proceedings of the Royal Society of London Ser. A* 229, 317-345.
- [24] Markos Papageorgiou, "Some remarks on macroscopic traffic flow modeling", Elsevier Science Ltd., Vol. 32, No. 5, pp. 323 to 329, 1998
- [25] Nott, M. (2005). "Teaching Brownian motion: demonstrations and role play". *School Science Review*, 86, 18-28.
- [26] Sethna J. P., "Statistical Mechanics Entropy, Order Parameters and Complexity", ISBN13: 9780198566779.
- [27] Van Dorp P. and Groen F.C.A. (2008). "Feature-based human motion parameter estimation with radar". *IET Proc. on Radar, Sonar, and Navigation*, 2 (2), 135-145.
- [28] Van Dorp, P. and Groen, F.C.A. (2003). "Human walking estimation with radar". *IET Proc. on Radar, Sonar, and Navigation*, 150 (5), 356-365.
- [29] Zhang, H. (1998). "A theory of nonequilibrium traffic flow". *Transportation Research B*, 32:485-498.